

**NASA TECHNICAL
MEMORANDUM**

NASA TM X- 67974

NASA TM X- 67974

**CASE FILE
COPY**

THE EFFECT OF ROCKET PLUME CONTAMINATION ON THE OPTICAL
PROPERTIES OF TRANSMITTING AND REFLECTING MATERIALS

by John R. Jack, Ernie W. Spisz, and John F. Cassidy
Lewis Research Center
Cleveland, Ohio

TECHNICAL PAPER for presentation at
Tenth Aerospace Sciences Meeting sponsored by
the American Institute of Aeronautics and Astronautics
San Diego, California, January 17-19, 1972



THE EFFECT OF ROCKET PLUME CONTAMINATION ON THE OPTICAL PROPERTIES OF TRANSMITTING AND REFLECTING MATERIALS

by John R. Jack,* Ernie W. Spisz,** and John F. Cassidy**
National Aeronautics and Space Administration
Cleveland, Ohio

Abstract

The preliminary results of plume contamination from a 5-pound thrust single-doublet, bipropellant rocket engine on the transmittance of quartz and the reflectance of a silicon monoxide overcoated aluminum mirror have been presented. Changes in quartz transmittance were found to be significant and were due to both absorption and scattering effects. Contaminant absorption effects were predominant at the short wavelengths and scattering effects were greatest in the visible wavelengths. Measured changes in mirror reflectance were due primarily to contaminant absorption. Scattering effects were found to be as much as 9 percent of the total reflected energy from the mirror. There were no noticeable chemical or erosion effects on either the quartz or the front surface mirror.

Introduction

The successful completion of any space mission requires that the space vehicle, its many system components, and its experimental packages all be maintained within certain prescribed specifications. In general, the specifications depend upon the space environment as well as the materials used, and the stability of the optical properties in the operational environment.

For a number of years the Lewis Research Center has been investigating the optical properties of various metals⁽¹⁾, paints and coatings⁽²⁾ primarily in the low temperature range from 100° to 500° K. More recently, however, our endeavors have been directed towards investigating the effects of the local spacecraft environment (such as rocket plume impingement and waste gas venting) on optical properties. For long-term missions it is necessary to control the vehicle orientation by means of small attitude control thrusters. As a result, the exhaust products of these engines may present a serious contaminating source for such things as thermal control materials, optical sensors, and solar cell arrays, to name a few. These sources of contamination may or may not be of importance. The contamination effect is of concern only when the functional thermal or optical property of a material of interest is measurably altered. For example, it is well established that optical sensors or imaging devices are particularly vulnerable to very thin film contamination that can absorb critical wavelengths or cause off-axis radiation to be scattered into their optical path. As a result, the degree and severity of rocket plume contamination under fairly realistic space simulation must be determined for a variety of materials.

The purpose of this paper is to present preliminary results for the effect of contamination

* Head, Environmental Physics Section.

** Aerospace Research Engineer.

due to rocket plume exposure on the spectral transmittance and absorptance of a fused quartz sample and the reflectance of a silicon monoxide overcoated aluminized mirror sample.

Experiment

The experimental program was carried out in the Lewis Research Center's 6- by 12-foot liquid helium-cooled space simulation chamber described in reference 3. The rocket engine and the test samples are located in this facility as shown in figure 1. The thruster being used is a scaled 5-pound thrust version of the R-1-D MOL reaction control system thruster (Marquardt Co.). This engine is a pressure-fed, bipropellant, single doublet unit with a stainless steel radiation-cooled nozzle. The fuel is MMH and the oxidizer is N₂O₄. Both were maintained at a temperature of 20° C. A pulsed firing mode typical of a proposed Skylab duty cycle was used. This operation mode included a firing time of 50 milliseconds, an off-time of 100 milliseconds, and a train of 4 pulses. The following table lists the primary engine design and nominal performance features.

Table I

- (a) Dribble volume oxidizer manifold = 0.00058 in.³
- (b) Dribble volume fuel manifold = 0.00113 in.³
- (c) Injector = Single doublet
- (d) Oxidizer injector orifice diameter = 0.0186 in.
- (e) Fuel injector orifice diameter = 0.0158 in.
- (f) L* = 4.5
- (g) Nozzle throat area = 0.0298 in.²
- (h) Nozzle area ratio = 39.2
- (i) Nozzle contraction ratio = 4.2
- (j) Oxidizer-fuel ratio = 1.6
- (k) Fuel and oxidizer valve opening time = 8 msec
- (l) Fuel and oxidizer valve closing time = 10 msec
- (m) Thrust = 5 lb
- (n) Specific impulse = 286 sec
- (o) Total flow rate = 0.0175 lb/sec
- (p) Combustion chamber pressure = 100 psi

Proper simulation is necessary if useful plume contamination data are to be obtained. Reaction control thrusters typically operate with a pulsed-mode duty cycle of 50-200 milliseconds of firing time and a similar period between firing pulses. The number of pulses during a given firing period generally varies from 2 to 20. Simulation chambers which use conventional vacuum systems consisting of mechanical and diffusion pumps along with liquid nitrogen cryopanel experience rapid decay in simulation pressures during such a firing period because of the limited pumping capability of such systems. This introduces serious simulation problems and can compromise the accuracy of the contamination data that are obtained from such facilities. Early cryopumping studies in the Lewis Research Center's liquid helium-cooled facility showed two significant advantages of this facility over the conventionally pumped space chambers. First, large

E-6632



amounts of room temperature hydrogen (3 liters/sec at standard conditions) could be cryopumped at a pressure of 3×10^{-5} torr. Second, the amount of hydrogen that could be cryopumped was increased by the addition of condensible gases⁽³⁾. Since the exhaust products of a bipropellant engine using MMH/N₂O₄ contains hydrogen as well as conventional and condensible gases such as H₂O, CO₂, CO, and N₂, it was expected that these condensible gases would provide additional cryopumping of the hot hydrogen gas. Rocket plume pumping tests performed in this facility show that starting with an initial pressure of 2×10^{-9} torr, a 50 millisecond firing of the 5-pound thrust, bipropellant thruster increases the ambient pressure only to 2×10^{-5} torr. Subsequently the ambient pressure was cryopumped very quickly back to the 2×10^{-9} torr level within 100 milliseconds. These results established that good space simulation could be achieved if the minimum time between firing pulses was 100 milliseconds.

Rocket engine design and performance characteristics can also strongly influence the formation, type, and character of the contamination. Design considerations such as the volume between the valve seats and the injector face (dribble volume), propellant flow distribution over the face of the injector, engine and propellant temperatures, valve timing characteristics, and the shape of the combustion chamber are all parameters that must be considered. In addition, the pulse firing mode of rocket engines introduces special concerns which are probably of the utmost importance in considering plume contamination. Pulse mode operation is inefficient because start-up and tail-off times are relatively large compared to the total pulse time. During these transients, unreacted fuel and oxidizer, and the intermediate products of combustion are formed. Also rapid valve response can form hydraulic pressure waves in the propellant flow system which can cause a pulsing-type flow having an approximate duration equal to the total firing time. If the fuel or oxidizer valves lead or lag each other, these transients can combine with the hydraulic pulsing and the start-up and shut-down transients and cause nonuniform oxidizer/fuel ratios which vary with time and position in the plume. All of these variables cannot be considered in a single experimental program but their importance and possible influence on contamination must be appreciated.

Ambient pressure instrumentation within the cryopumped facility consists of a buried collector hot-ionization gauge and a mass spectrometer. Each instrument has an electrometer connected directly to the collector. The total response time of the electrometer and the buried collector gauge is 100 microseconds per decade. The response time of the nude mass spectrometer and the electrometer is 200 milliseconds to scan the mass number range from 2 to 200.

For the specific experiment described herein, the thruster was fired in a 4 pulse train mode consisting of 218 trains or 872 firing pulses. Each pulse consisted of a firing period of approximately 50 milliseconds, and an off time of 100 milliseconds. The samples were exposed to propellant exhaust products for a total exposure time of approximately 44 seconds. The duration of the test firings occurred over a period of approximately 20 days.

Eight samples were mounted within the test chamber on the temperature-controlled (approx. 20° C) test pallet shown in figure 2. Four of the test samples are 5 mm thick fused quartz (Amersil T-08 commercial grade) samples. Two of the samples are 3 mm thick fused silica (Corning 7940) samples. The remaining two samples are silicon-monoxide-overcoated aluminized mirrors. All samples are approximately 2.5 cm in diameter. The samples are mounted in aluminum cup-shaped holders which are mounted flush with the test pallet surface so that only the top surfaces of the sample are exposed to the thruster discharge.

Spectral measurements of the optical properties of the samples were made both before and after exposure of the samples to the thruster discharge. The after-exposure spectral measurements were made during a period of 3 to 30 days after the samples were removed from the test facility. No special precautions were taken during this time to insure that the surface contamination layer would not change. The samples however were handled as carefully as possible but were stored only at room conditions.

Two different spectrometers were available for making bench-type spectral transmittance measurements. These are (1) Gier-Dunkle magnesium oxide-coated integrated sphere with a lithium fluoride prism monochromator^(4,5), and (2) a 1-meter, 15 degree Robin mount ultraviolet scanning spectrometer with a 590 grooves per millimeter concave grating blazed at 0.15 micrometers⁽⁶⁾. Integrating sphere transmittance measurements were made by the sample-in/sample-out technique with the sample mounted at the inlet port of the integrating sphere. Transmittance measurements are made over the wavelength range from 0.25 to 2.2 micrometers. Integrating sphere absorptance and reflectance measurements were made by mounting the sample in the center of the integrating sphere. The uv spectrometer was only used to make transmittance measurements at the shorter wavelengths from 0.2 to 0.6 micrometers. These measurements were also made by the sample-in/sample-out technique with the sample located at the entrance port of the spectrometer.

Results

The results to be presented are limited to the fused quartz sample (FQ-A) and the mirror sample M-A. The data for these two samples are typical and represent the general character of the effect of contamination at all plume locations illustrated in figure 2.

Photographs of the resulting contamination on both the fused quartz sample FQ-A and mirror sample M-A are shown in figure 3. The contamination can be qualitatively described as composed of small, discrete, colorless and transparent droplets. The general character of the contamination on the two samples is somewhat different. On the fused quartz sample, the contamination consists mainly of large irregular shaped droplets with mean diameters in the 20 to 500 micrometer range. Much of the quartz surface however appears to be uncontaminated and unaffected by the exposure to the engine exhaust. On the mirror sample the contamination occurs in generally the same droplet size but the droplets are all very nearly circular (probably hemispheri-



cal) in appearance except for the largest droplets which are oval. In addition, the surface area between the larger droplets is covered with many small droplets whose diameters are less than 10 micrometers. The entire surface of the mirror sample appears to be affected to some extent by the exposure to the engine exhaust. It should be noted that the droplet distribution on both samples may be affected to some degree by gravity because of the orientation of the experiment.

The transmittance measurements of the fused quartz sample, before and after a total exposure of 44 seconds of pulse mode firing are shown in figure 4 for the wavelength range from 0.2 to 0.6 micrometers. The change in transmittance as measured by the two different spectrometer measurements is shown in figure 5. Data are not presented at wavelengths greater than 0.6 micrometer because (1) measurements could not be made with the uv spectrometer beyond 0.6 micrometer and (2) no noticeable change in total transmittance was indicated from the integrating sphere measurements. As can be noted from figures 4 and 5, the after-exposure transmittance measurements obtained with the two spectrometer systems are different. (No noticeable difference was noted between the measurements for the uncontaminated samples.) The primary reason for the difference is that the two spectrometers make different transmittance measurements. The transmittance that is measured with the integrating sphere is a hemispherical transmittance in that all of the energy passing through the sample is measured. The transmittance that is measured with the uv spectrometer is a more directional (or specular) measurement in that not all of the energy transmitted by the sample is measured. Only the transmitted energy that is contained within a small solid angle aligned along the optical axis is measured. Thus, the difference between the measurements of the two instruments is basically due to the scattering effect of the contamination. The data from both instruments show the increasing effect of the contamination with decreasing wavelength.

The changes measured with the integrating sphere are due to absorption by the contaminating layer and changes in the front surface reflection of the sample. The incident energy that is absorbed by the contaminated sample can be determined explicitly by mounting the sample in the center of the integrating sphere. In figure 6, the absorptance is compared with the change in the transmittance (fig. 5) as measured with the integrating sphere. The curves are very similar and indicate that contaminant absorption accounts for the major portion of the transmittance change. (Absorption by a clean fused quartz has been measured and is negligible.) However, there does appear to be some change in the front surface reflection due to the contaminants (accounting for the remaining difference between the two curves).

Also shown in figure 6 is the difference between the change in transmittance as measured by the two different spectrometers. The difference is essentially the "scattering" effect of the contaminant. The effect is small at the short wavelengths but increases with wavelength and becomes the predominating degradation mechanism in the visible wavelength range.

Figure 7 shows the effect of the contaminant

on both the hemispherical reflectance and the diffuse reflectance of a silicon-monoxide overcoated aluminum mirror as measured by the integrating sphere spectrometer system. The diffuse reflectance measurement can be used as a qualitative indication of the change in specularity of the mirror reflectance. The diffuse reflectance measured with the integrating sphere is the reflected radiation that is not included in a 15 degree solid angle normal to the sample for radiation at normal incident. For the wavelength range from 0.35 to 1.6 micrometers, the diffuse reflectance is approximately constant at a value of 0.09. For wavelengths less than 0.3 micrometers the diffuse reflectance decreases with decreasing wavelength similar to the trend exhibited by the effect of scattering on transmittance. For a clean mirror, the diffuse reflectance is nominally zero as is the scattering on a clean uncontaminated quartz sample.

The change in the hemispherical reflectance of the mirror due to contamination is shown in figure 8. This change in reflectance is equivalent to the change in absorptance attributed to the contaminant. The effect of the contaminant increases with decreasing wavelength and is similar to the absorptance curve obtained from measurements on the fused quartz samples. The change in reflectance however is significantly greater than the measured absorptance for the transmitting sample due to the multiple pass of the incident energy through the contaminant on the mirror surface. The significance of this comparison is that, although the contaminant and its distribution may be identical, its absorption effects may be radically different depending upon the optical element being used.

Concluding Remarks

The preliminary results of plume contamination from a 5-pound thrust, single-doublet, bi-propellant rocket engine on the transmittance of quartz and the reflectance of a silicon monoxide overcoated aluminum mirror have been presented. Changes in quartz transmittance were found to be significant and were due to both absorption and scattering effects. Contaminant absorption effects were predominant at the short wavelengths and scattering effects were greatest in the visible wavelengths. Measured changes in mirror reflectance were due primarily to contaminant absorption. Scattering effects were found to be as much as 9 percent of the total reflected energy from the mirror. There were no noticeable chemical or erosion effects on either the quartz or the front surface mirror.

It should be recognized that the conclusions which have been drawn from this data apply only to the very specific set of experimental conditions under which the contaminant was formed and the manner in which the measurements were made. Probably the most serious limitation regarding the data is the usefulness of the "on the bench" rather than in situ measurements. The deposited material which forms on the sample surface is accepted as being hygroscopic. The contaminant as observed in the laboratory exists as clear, transparent, liquid droplets due to its hygroscopic characteristics. It is not known whether the droplet form is the actual state of the contami-



nant as it exists in the simulator. Even though water is one of the exhaust products from the engine, it is possible that the in situ contaminant is significantly different in appearance and therefore causes different changes in the optical properties of materials than those which have been measured.

There also exists two interactions between the plume and the sample pallet that may affect the amount and possible type of contaminant encountered. First, there may be a gravity effect and second, the pallet configuration used does not simulate a large extended spacecraft surface. As a result the boundary layer above the pallet can be considerably different than that which exists on an actual spacecraft configuration.

A first attempt has been made to determine the effectiveness of the space simulator by placing witness samples in the simulator that were not exposed directly to the plume. The witness samples were also found to be contaminated but to a much lesser degree. The absorbance change due to this contaminant is negligible but the effect on scattering may be important.

One final limitation associated with the actual magnitude of the optical property change is concerned with the nonuniformity of the contaminant on the sample surface. For the small slit widths that are used for the spectrometer measurements (especially the uv spectrometer) large differences can be noted in the data depending upon the sample area that is viewed.

Future experiments are being planned to reduce these limitations and to provide quantitative data on the contamination effects to be expected under realistic space simulation.

Acknowledgments

The authors would like to acknowledge the efforts of Robert Bowman and Perry Campbell who assisted in obtaining and analyzing the contamination data.

References

1. Jack, J. R. and Spisz, E. W., "Thermal Radiative Property Measurements Using Cyclic Radiation," TN D-5651, 1970, NASA, Cleveland, Ohio.
2. Spisz, E. W. and Jack, J. R., "Thermal and Radiative Property Measurement of Thermal Control Coatings by Cyclic Radiation," TN D-6316, 1971, NASA, Cleveland, Ohio.
3. Cassidy, J. F., "Space Simulation Experiments on Reaction Control System Thruster Plumes," proposed NASA Technical Note.
4. Edwards, D. K., Gier, J. T., Nelson, K. E., and Roddick, R. D., "Integrating Sphere for Imperfectly Diffuse Samples," Journal of the Optical Society of America, Vol. 51, No. 11, Nov. 1961, pp. 1279-1288.
5. Anon., "Instruction Manual - Perkin Elmer Infrared Equipment," Vol. 3A, Perkin Elmer Corp., Norwalk, Conn., 1956.

6. Anon., "Model 78-751, 1 meter, 15° Robin Mount Vacuum Ultraviolet Scanning Spectrometer, Engineering Publ. No. 78-751, July 1966, Jarrell-Ash Co., Waltham, Mass.



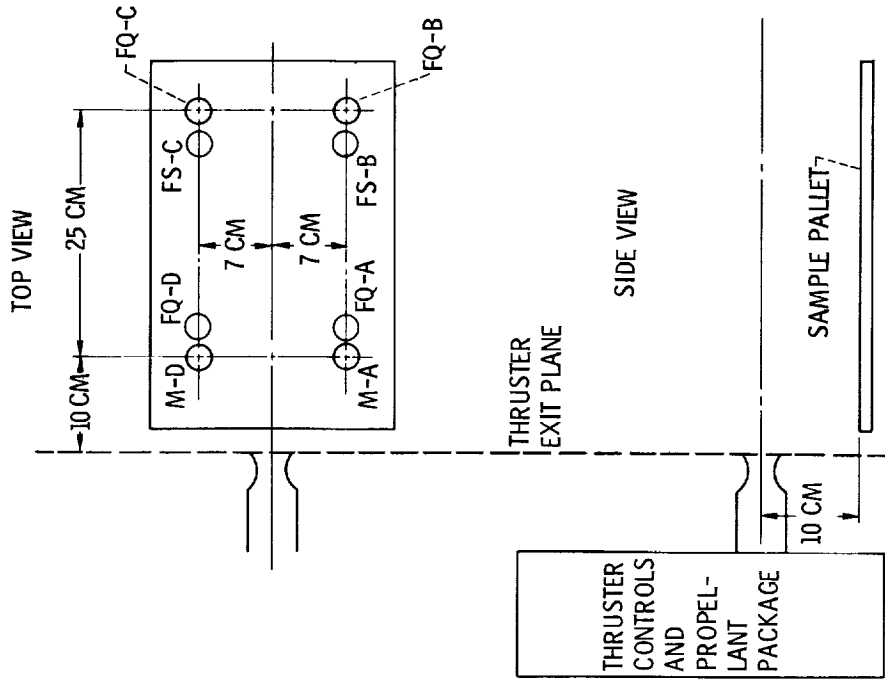


Figure 2. - Sample location. M, silicon monoxide overcoated aluminum mirror; FQ, fused quartz samples (5 mm thick) (Amersil Inc. commercial grade T-08); FS, fused silica samples (3 mm thick) (Corning Glass Works, standard grade 7940).

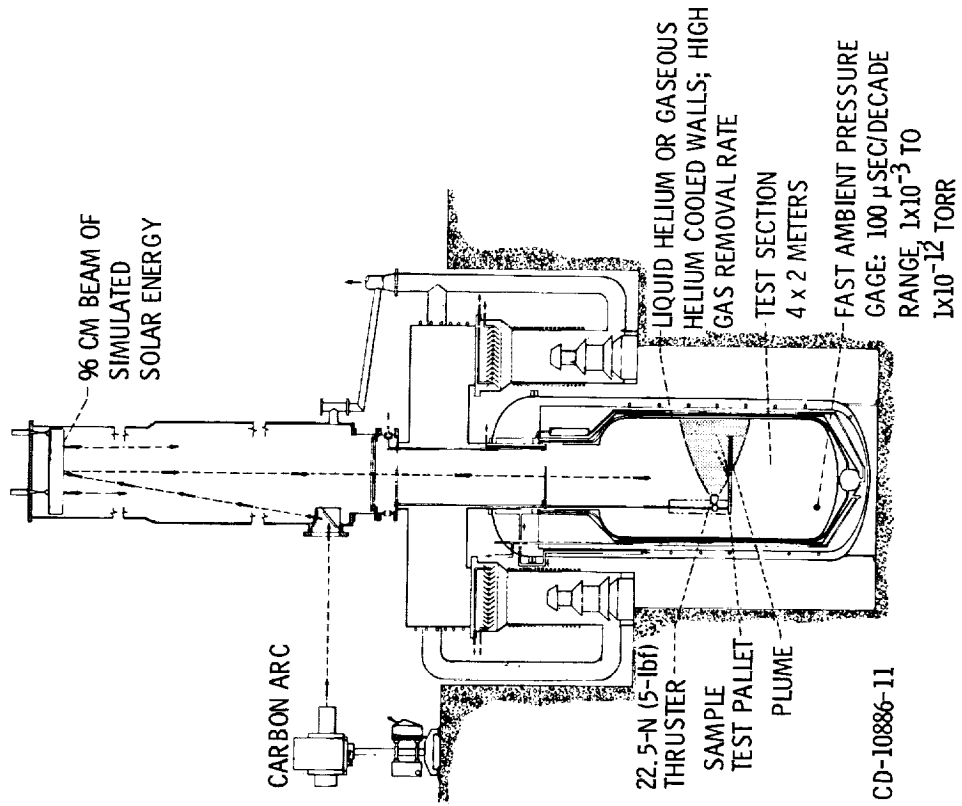
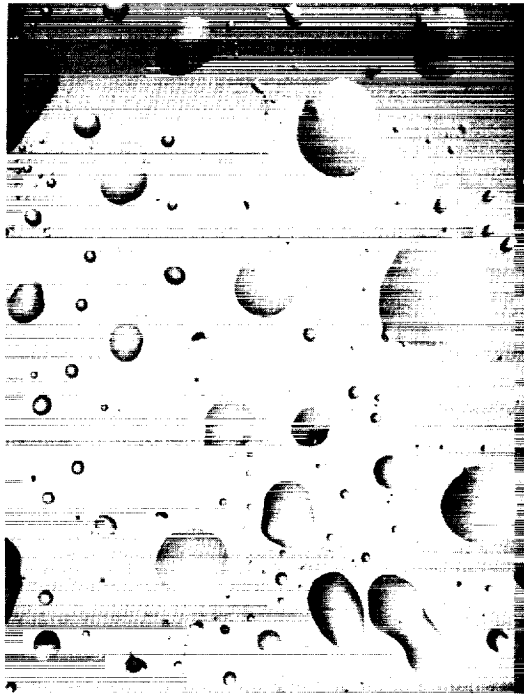
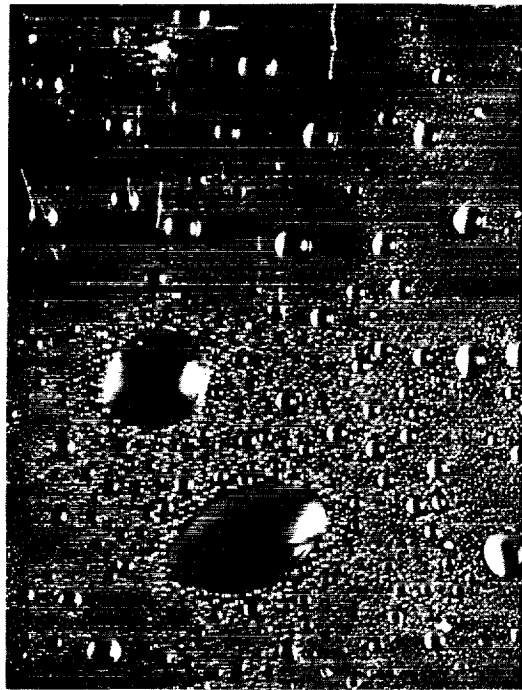


Figure 1. - In-situ rocket plume effects facility.





(a) Fused quartz sample, FQ-A.



(b) Aluminum mirror sample, M-A.

Figure 3. - Photographs of contaminated samples. Field of view, 2 mm x 2 mm. Magnification X40.



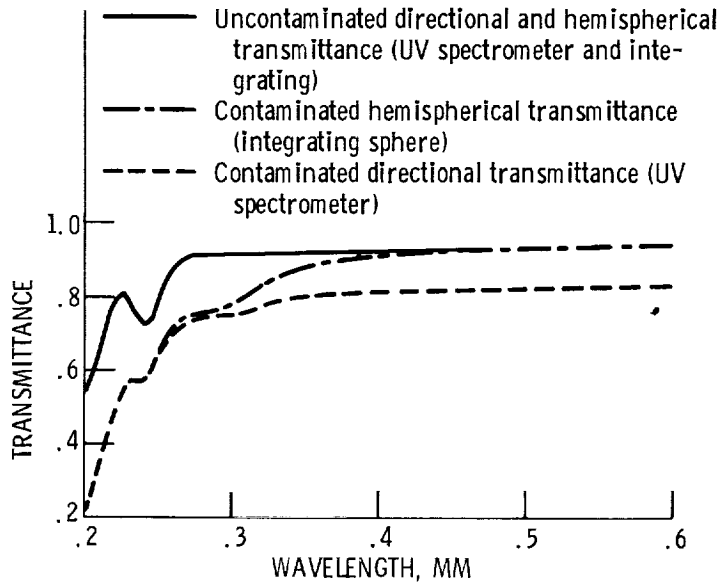


Figure 4. - Effect of thruster contaminant on transmittance of fused quartz sample FQ-A.

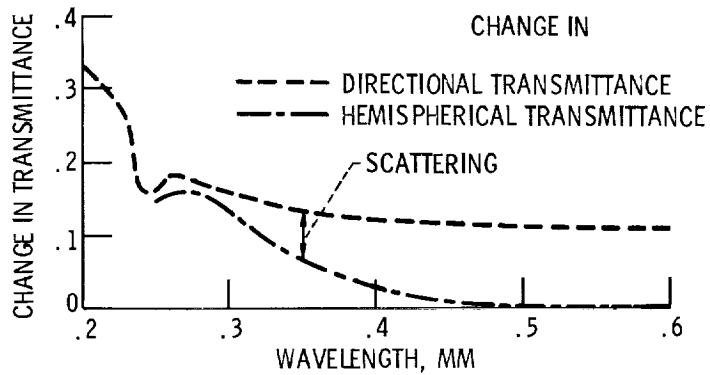


Figure 5. - Change in transmittance due to contamination on sample FQ-A.

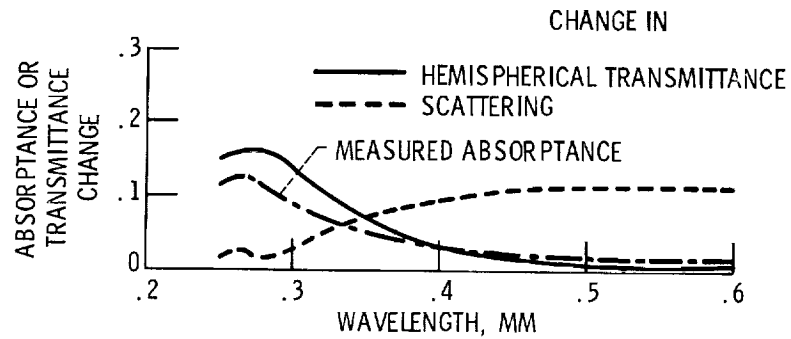


Figure 6. - Effect of contamination on fused quartz sample FQ-A.



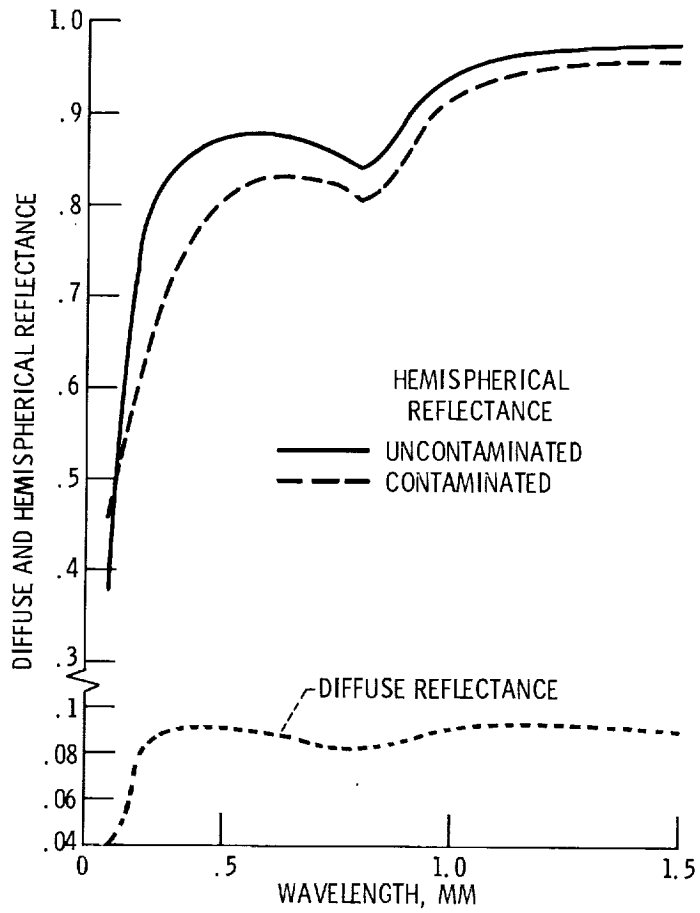


Figure 7. - Effect of thruster contamination on the reflectance of mirror sample M-A.

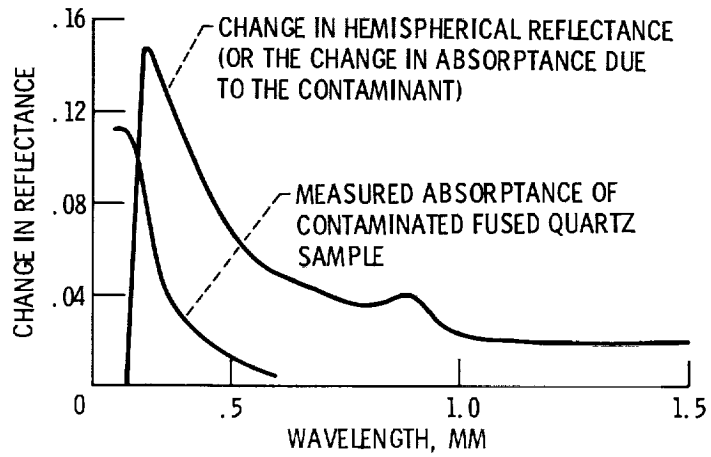


Figure 8. - Change in reflectance of mirror sample M-A due to thruster contamination.

